JOURNAL OF MAGNETIC RESONANCE **124,** 410–419 (1997)
ARTICLE NO. MN961044

^{1}H NMR Measurements of Wet/Dry Ratio and T_1, T_2 Distributions in Lung

MOHAMMADREZA ESTILAEI,* ALEX MACKAY,* CLIVE ROBERTS,† AND JOHN MAYO‡

*Department of Physics, University of British Columbia, Vancouver, Canada V6T 1Z1; †UBC Pulmonary Research Laboratory, University of British Columbia, Vancouver, Canada V6Z 1Y6; and ‡Department of Radiology, Vancouver Hospital, Vancouver, Canada V5Z 1M9

Received May 13, 1996; revised October 18, 1996

Proton-magnetic-resonance measurements have been carried out on juvenile porcine peripheral lung parenchyma. The free-induction-decay signal contained a motionally restricted component which decayed in a few tens of microseconds and a mobile component with a T_2 time greater than 1 ms. The average second moment, M_2, for the motionally restricted signal was found to be $3.42 \pm (0.25) \times 10^9$ s^{-2}. The T_2 distribution for the mobile signal consistently showed four resolvable components of T_2 range: 2–6, 10–40, 80–110, and 190–400 ms. The 2–6 ms component was present in a fully dehydrated preparation and was therefore assigned to a nonaqueous lung constituent. The motionally restricted FID component had a $T_1 = 0.772 \pm 0.11$ s and the mobile component had a $T_1 = 0.967 \pm 0.02$ s. The hydrogen content per unit mass for lung parenchyma and water were estimated in two ways: (1) on the basis of chemical content and (2) on the basis of comparison of restricted and mobile signals to the gravimetric (G) water content for a lung sample studied at a wide range of water contents. Lung wet/dry weight ratios were estimated from the free-induction decays and compared with gravimetric measurement. The ratio of $(\text{wet/dry})_{\text{NMR}}/(\text{wet/dry})_{\text{G}}$ was 1.00 ± 0.08 and 1.00 ± 0.05 for the two methods of estimation.

INTRODUCTION

The proton-magnetic-resonance signal from lung tissue is quite complex, arising from distinct water compartments and different molecular constituents. A typical deflated excised lung sample consists of collagen, elastin, and ''whole cells'' in water. Whole cells, in turn, have an intricate composition consisting of lipids, membrane proteins, cytoplasmic proteins, and metabolites (*1*). The interpretation of the ^{1}H NMR signal from lung is complicated by a number of factors, including magnetic susceptibility variation (*2*), dipolar line broadening (*2, 3*), diffusion (*4, 5*), heterogeneity (*4, 6*), and paramagnetic solutes. Nevertheless, several types of useful information are available from the ^{1}H NMR signal.

Since alteration in lung water content is an important feature in a number of lung diseases, it would be quite advantageous to accurately measure the water content in a noninvasive/nondestructive manner. For this reason, a series of studies have been conducted on the determination of water content both *in vivo* and *in vitro* (*7–14*). This paper presents an analysis on the entire ^{1}H NMR signal of lung tissue *in vitro.* Because the NMR signal can provide a direct measure of lung-tissue water, MRI is a good method for investigation of inflammatory and degenerative diseases (*15, 16*).

Two significant NMR properties of many tissues including lung are spin–spin relaxation time, T_2, and spin–lattice relaxation time, T_1, which are measured by the CPMG pulse train and inversion-recovery sequence, respectively (*17–19*). In lung or any biological tissue, protons exist in a variety of different environments, giving rise to a wide range of relaxation times. Therefore, the measured decay curve is a sum of contributions from all spins which may have sampled different environments during the course of the experiment. As a result, these measurements should enable us to obtain information on water distribution and tissue pathology. Previous studies have demonstrated that pulmonary injury can be characterized by changes in the tissue's relaxation times (*20–27*). The value of T_2 has been shown to be a more sensitive and useful parameter for pulmonary edema than T_1 (*14, 15, 23*).

In this study, ^{1}H NMR measurements on lung were carried out with a solid-state NMR spectrometer which had both a high signal-to-noise ratio (S/N) and a short dead time ($\approx$10 μs). These characteristics made it sensitive to the complete proton signal from lung tissue. For comparison, conventional clinical MRI scanners are sensitive only to protons with T_2 values greater than about 10 ms.

The total ^{1}H NMR signal of a typical lung tissue consists of a fast-decaying component, lasting approximately 30 μs, and a slow-decaying part which persists over 10 ms or longer. The latter signal arises from water and mobile protons associated with cytoplasmic proteins and metabolites which undergo rapid isotropic motion, averaging dipolar interactions to zero (*1*). The rapidly decaying component can be characterized by the second moment of its lineshape which provides us with insight into the dynamic structure of the solid component of lung (*28, 29*). The mobile signal

1090-7807/97 $25.00

can be characterized by its T_1 and T_2 relaxation times which relate to the microscopic tissue environment.

A large number of diagnostic changes in lung tissue are characterized by alteration in wet/dry ratio. The relative signals from water and nonaqueous tissue may be used to estimate the wet/dry ratio of the lung samples. In the absence of T_1 and T_2 weighting, NMR signal intensities are proportional to the number of contributing protons. Therefore, to estimate wet/dry ratios from the free-induction decay, we require values for the hydrogen content per unit mass for lung tissue and for water. Two methods were employed to estimate lung proton density: (1) a calculation based upon chemical content and (2) a measurement based upon the NMR signal from a lung sample which was dehydrated incrementally. For partial chemical characterization, the collagen content of several of the lung samples was obtained by hydroxyproline analysis.

The initial aim of our research project was to understand the nature of the entire ^{1}H NMR signal of lung and to measure lung water content quantitatively both *in vitro* and *in vivo*. The ultimate goal is to characterize pathologic processes in the lung by alterations in the water content and relaxation properties of the ^{1}H NMR signal. This should enhance the diagnostic potential of lung parenchymal MRI, perhaps allowing differentiation of potentially reversible inflammatory infiltrates from fixed fibrotic lung changes.

MATERIALS AND METHODS

Samples

Twenty-one deflated excised samples of volume about 1 cm^3 of peripheral lung from four different normal juvenile pigs were sealed in sample tubes of 1 cm diameter. The pigs had been euthanized with a sodium pentabarbitol overdose and then exsaguinated passively by cutting the abdominal aorta before lung excision. The animal experimental protocol was approved by the institutional ethics review board.

Hydroxyproline

To determine tissue collagen content, the collagen-specific amino acid hydroxyproline was assayed in 15 samples. Tissue samples were hydrolyzed in 6 ml HCl overnight and under nitrogen at 105°C. Hydrolyzates were neutralized and assayed for hydroxyproline, applying the method of Stegemann and Stalder, using known amounts of purified type I collagen as standards (*30*). Hydroxyproline values of each sample were converted to collagen content, based on an average collagen content of 1/7 hydroxyproline by weight.

NMR Equipment

Proton NMR measurements were carried out on a modified Bruker SXP 4-100 operating at 90 MHz. Data acquisition and analysis were carried out on a system including a locally built pulse programmer (*31*), a Rapid Systems digitizer, and an IBM-compatible computer. The ^{1}H NMR spectra measurements were performed on a 300 MHz Varian XL-300 spectrometer. All the experiments were done at 24°C.

Free-Induction-Decay Measurements

A modified version of the free-induction-decay pulse sequence was used to determine the wet/dry ratios and to measure the moments. This pulse sequence was applied to distinguish the fast-decaying nonaqueous signal from the water and mobile nonaqueous signal. The pulse sequence is represented by

$$90^\circ_{0^\circ} - \frac{\tau}{2} - (180^\circ_{90^\circ} - \tau)_n,$$

where $n = 8$, $\tau = 200$ μs, and the repetition time was 10 s. The subscripts indicate phase shift of the pulses relative to the reference signal. The 180° pulses were applied to refocus phase dispersion in the mobile signal due to magnetic field inhomogeneity. The duration of the 90° pulse was between 1.8 and 2 μs. The fast-decaying signal, from dipolar-coupled protons of the sample, was fitted to a moment expansion equation of the form

$$S(t) = (S_0 - L_0)\left(1 - M_2\frac{t^2}{2!} + M_4\frac{t^4}{4!} - M_6\frac{t^6}{6!}\right) + L_0, \quad [1]$$

where M_2, M_4, and M_6 are the second, fourth, and sixth moments of the total proton lineshape (*18*) and S_0 and L_0 are the signal intercepts at zero time from the total and mobile signals. It was assumed that the mobile signal, L_0, was constant over the duration of the motionally restricted signal. S_0 and the three spectral moments were estimated by fitting Eq. [1] to 20 FID points between approximately 12 and 32 μs (see the inset of Fig. 1) using a nonlinear functional optimization program to minimize χ^2 (*32*). Eight points per echo were averaged to make up a mobile-signal decay curve for T_2, which was fitted by a simple monoexponential fitting algorithm to estimate the constant L_0. The spectral moments obtained above relate to the total NMR signal. To obtain the second moment for the motionally restricted component alone, the value from Eq. [1] was divided by $(S_0 - L_0)/L_0$ in order to remove the contribution from the mobile signal which was assumed to possess zero M_2.

Spin–Spin Relaxation

The Carr–Purcell–Meiboom–Gill (CPMG) pulse train was applied to each sample to acquire the T_2 decay curve. The sequence is represented by

$$90^\circ_{0^\circ} - \frac{\tau}{2} - (180^\circ_{90^\circ} - \tau)_n,$$

where $n = 4230$. A recycle time (TR) of 10 s allowed reequilibration of magnetization. Totals of 250 and 2500 scans were accumulated for the wet and fully dehydrated samples, respectively. The sequence was repeated with $\tau =$ 100, 200, 400, 600 μs in order to investigate the dependence of the decay curve upon echo spacing. To calculate the T_2 distribution, four points per echo were averaged and 736 echo amplitudes were collected from the echo train to obtain the transverse magnetization decay curves. These curves could be represented by the sum of several components,

$$S(t) = \sum_{i=1}^{m} S_i e^{-t/T_{2(i)}}, \qquad [2]$$

where S_i is the relative magnetization of each component, proportional to the number of protons, and T_{2i} are the component relaxation times.

Spin–Lattice Relaxation

A modified version of the inversion-recovery pulse sequence was employed which is represented by

$$90^\circ_x - \text{TR}$$

$$180^\circ_x - \tau - 90^\circ_x - \text{TR},$$

where the second signal was subtracted from the first to give a positive signal that decayed to zero at long τ. The recycle time TR of 10 s was selected for the wet samples. Thirty τ values (the range over which τ varied depended on T_1) were chosen in a geometric fashion from 500 μs to 5 s. Furthermore, the free-induction-decay curve was decomposed into two separate components to investigate the T_1 distributions for the motionally restricted and the mobile components. To acquire the total NMR signal, S_0 was estimated the same way as explained earlier for all the τ values to obtain a T_1 decay curve. For the mobile component, L_0 was estimated for all the τ values by fitting the FID curve, between 200 and 1800 μs, to a monoexponential algorithm. The T_1 decay curves for $S_0 - L_0$ and L_0 were analyzed with a nonnegative least-squares method (*33*) to determine the T_1 distributions for the motionally restricted and mobile components, respectively.

Dehydration

Following NMR measurements, all samples were weighed and then dried under vacuum at 55°C to constant weight in order to obtain their gravimetric wet/dry ratio. One additional sample was dehydrated incrementally by allowing evaporation of water under vacuum at room temperature. At each step, lung weight measurements were performed, using an accurate balance (Sartorius 2462) with sensitivity of 0.1 mg. A monotonic decrease in the mobile signals as well as the evolution of the T_2 distribution was observed. Finally, the samples were completely dried under vacuum at 55°C to constant weight.

Nonnegative Least-Squares Analysis of Relaxation

T_1 and T_2 relaxation curves were analyzed using a nonnegative least-squares algorithm (*33*). This method requires no a priori assumptions about the number of exponential components and amplitudes, m (see Eq. [2]). However, a large number of relaxation times must be specified. One hundred fifty geometrically scaled relaxation times from 0.0001 to 10 s were specified for spin–spin relaxation and 150 linearly scaled T_1 times from 0.001 to 10 s were used for spin–lattice relaxation. The algorithm puts nonzero amplitudes at a few of these times in order to minimize the misfit χ^2. Smooth distributions of relaxation times were generated by minimizing $\chi^2 + \mu A$, where A is the sum of squares of the amplitudes of the solution and χ^2 was increased by 3% above its minimum by increasing the regularization parameter μ.

RESULTS

Collagen Assay

Hydroxyproline assay experiments were conducted in order to determine the collagen content of each individual sample; the collagen content of the peripheral lung-tissue samples ranged from 13 to 41% of the dry weight.

Free-Induction-Decay Measurements

A typical FID from a lung sample is shown in Fig. 1. The 180° pulses were required in order to refocus phase dispersion due to magnetic field inhomogeneity. A rapidly decaying signal lasting approximately 30 μs was observed, corresponding to the motionally restricted component. Signals from water and mobile protons were observed lasting 10 ms or longer. S_0, the total NMR signal at $t = 0$, and L_0, the signal from water and mobile nonaqueous tissue at $t =$ 0, were obtained from fitting Eq. [1] to this curve.

The simplest way of obtaining quantitative information from the broad-line NMR signal received from the nonaqueous component of lung tissue is the method of moments. The most important moment for structural studies is the second moment. To determine the moments, the fast-decaying part of the signal, which has a shape determined by dipolar broadening, was fitted to Eq. [1] as shown in the inset of Fig. 1. The average M_2 value for the wet samples was about $3.42 \pm (0.25) \times 10^9$ s^{-2}. This value is similar to that obtained from other biological samples such as rhodopsin (*29*).

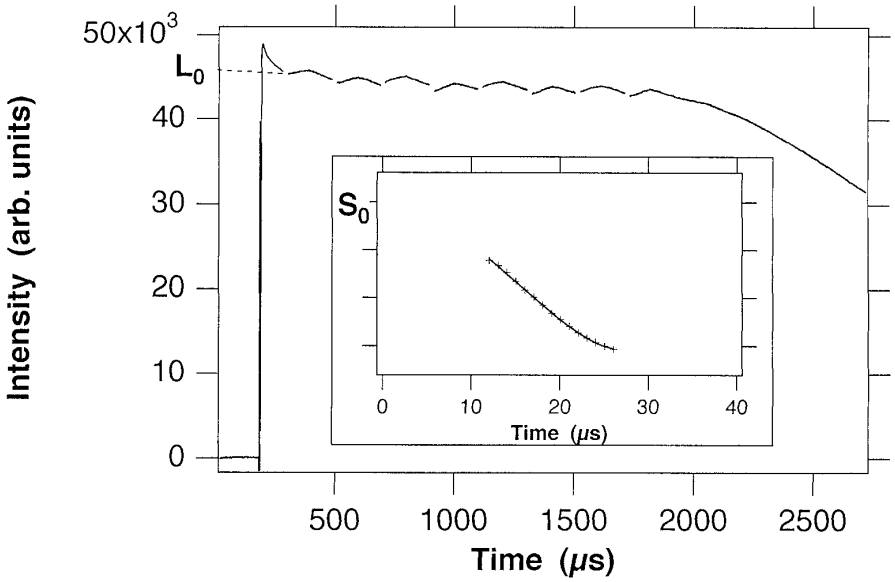

FIG. 1. A typical free-induction-decay curve from a lung sample. The gaps indicate the applied 180° pulses, $\tau = 200$ μs. The insert is the motionally restricted component fitted by the moments expansion.

Inversion-Recovery Measurements

Spin–lattice relaxation was measured in four lung samples. Inversion-recovery curves were fitted using the nonnegative least-squares algorithm (NNLS) to produce T_1 distributions for the motionally restricted and the mobile components. For both components, the decay curves were monoexponential. The former component had an average $T_1 = 0.772 \pm 0.11$ s and the mobile component had a T_1 of 0.967 ± 0.02 s. Since the T_1 values are relatively close to each other, there may have been an exchange of magnetization occurring between the two components. The T_1 values measured in this study were much shorter than the 10 s repetition times employed, indicating that the results were not corrupted by T_1 weighting. A more complete study of T_1 in lung tissue, including the effects of exchange between different spin groups, was carried out on mouse lung (*34*).

CPMG Measurements

To characterize the mobile fraction of the lung samples, the CPMG relaxation decay curve was acquired. The inset of Fig. 2 demonstrates that the CPMG decay curve was not a straight line on a semilog plot and hence could not be fitted by a single T_2 component corresponding to a single water environment. Figure 2 shows a typical NNLS discrete and smooth T_2 distribution for a mobile signal. Because of the inhomogeneous nature of the structure and biochemical composition of lung tissue, it may be more plausible to assume a smooth distribution for relaxation times. Also, the smooth fit is more robust in the presence of noise.

Four to five resolvable T_2 components were consistently obtained which were in agreement with the literature (*5*). These components had a range of 2–6, 10–40, 80–110, and 190–400 ms with average T_2 values of 4 ± 0.4, 35 ± 1.7, 93 ± 2.8, and 264 ± 28 ms. The largest component, which contained more than 75% of the total amplitude, was between 80 and 110 ms.

To have a better understanding of the motions responsible for the T_2 relaxation, four different values of echo spacing, τ, of 100, 200, 400, and 600 μs were applied in order to determine whether there were shifts or any other changes in the T_2 distribution. However, no changes were observed. This result indicated unambiguously that correlation times of 100 μs or longer do not play a role in the T_2 relaxation results.

Moisture Content

All 21 lung samples were weighed immediately before and after NMR measurements, and after drying to constant weight. The resulting mean gravimetric wet/dry ratio was 5.67 ± 0.10.

One lung sample was dehydrated incrementally to constant weight. The free-induction decay, the CPMG decay curve, and the sample weight were measured at each hydration level. Using Eq. [1], S_0, L_0, and M_2 were estimated as a function of sample hydration. Figure 3 shows that the second moment exhibited a twofold increase at low wet/dry ratios. Figure 4 shows the T_2 distribution at four hydration levels. We note that the T_2 value for the component with the shortest T_2 remained relatively constant; however, its amplitude increased at later stages of the dehydration process. This component was therefore assumed to be nonaque-

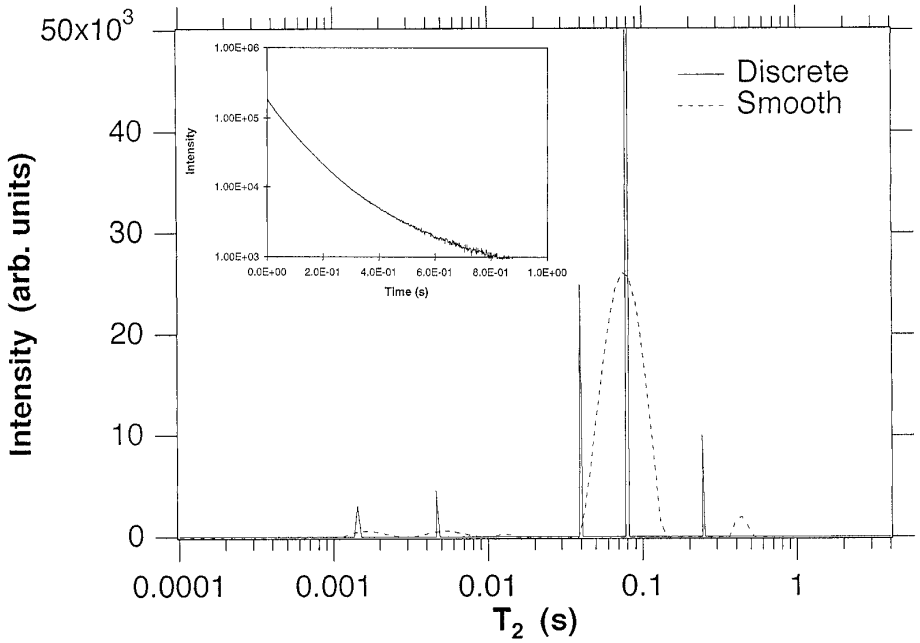

FIG. 2. Smooth T_2 distribution of mobile component (dashed line) and discrete distribution (solid line) from a lung sample. The inset is the T_2 magnetization decay curve from the CPMG sequence on a semilog plot, $\tau = 200$ μs.

ous. The amplitudes and the T_2 times for the other components decreased with decreasing moisture content and they were absent from fully dehydrated samples. The 300 MHz ^{1}H NMR spectra were measured on a wet and a fully dehydrated sample. For the wet sample, a peak was observed centered around 5.3 ppm which was assigned to water. After the sample was fully dehydrated under vacuum at 55°C, the spectrum contained a broad peak around 6.8 ppm. This peak was associated with nonaqueous mobile protons.

DISCUSSION

Collagen Content Measurements

Collagen is a major constituent of lung, representing from 13 to 41% of the weight of the samples used in this study. Collagens of different types are the major group of proteins in the lung and are present in all major structures, including airways, blood vessels, and the interstitium of lung paren-

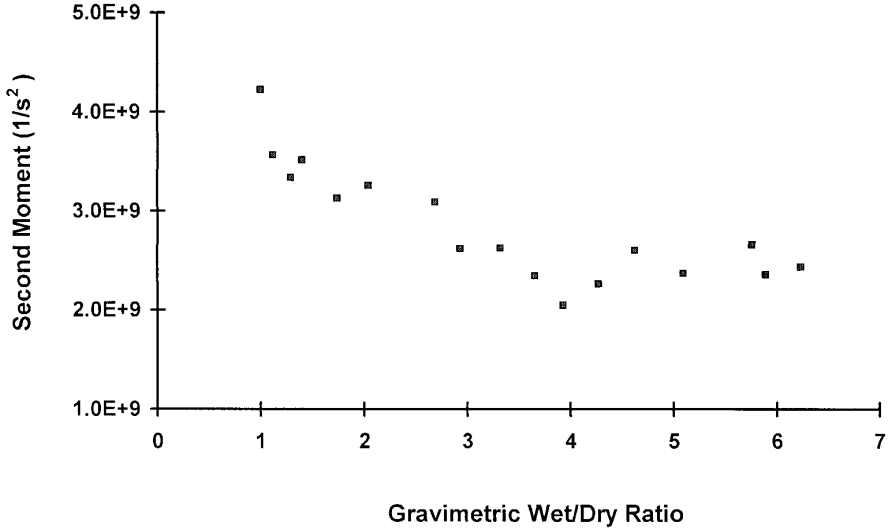

FIG. 3. The second moment (s^{-2}) plotted as a function of wet/dry ratio for one lung sample. A twofold increase was observed as the sample was dehydrated.

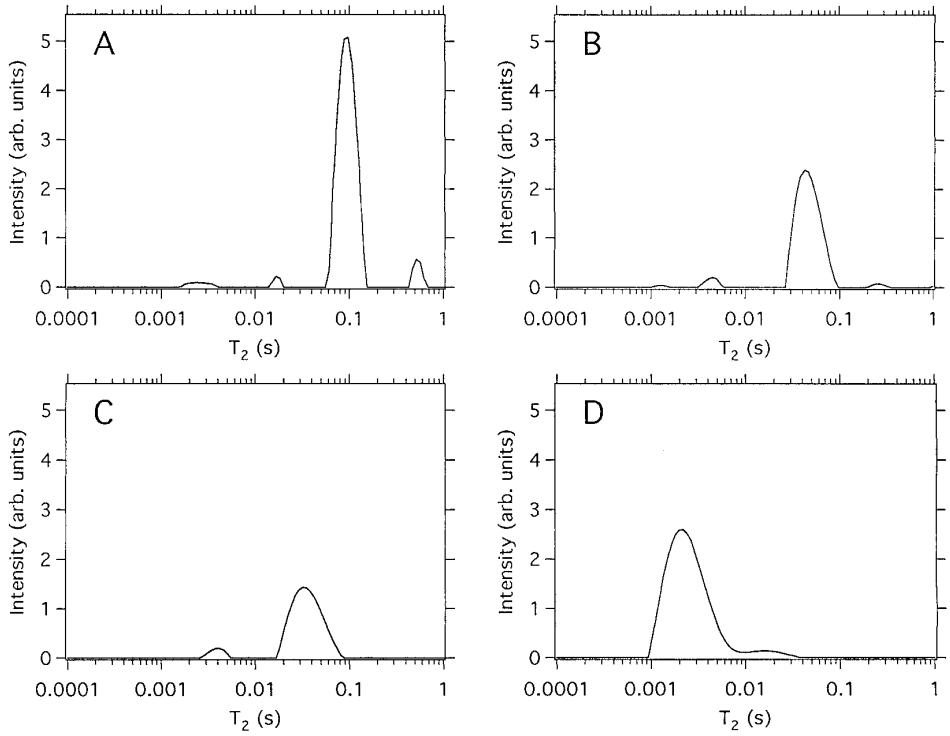

FIG. 4. The smooth T_2 distribution of the mobile signal from a lung sample at four different hydration levels: (A) For the fresh lung sample, wet/dry = 6.22, four resolvable components were obtained. (B) As the sample was dehydrated, wet/dry = 3.65, the four resolvable components were shifted toward lower relaxation times and their amplitudes decreased. (C) At wet/dry = 2.65, only two components remained. (D) For the fully dehydrated sample, wet/dry = 1.00, a component with an average T_2 of 4 ms remained.

chyma. Furthermore, characteristically, fibrotic tissue is believed to consist mostly of collagen. Therefore, it seemed worthwhile to investigate the dependence of the NMR properties, including motionally restricted and nonaqueous mobile signal intensities, M_2, T_2 amplitudes and times, and water content upon collagen content. Moreover, since collagen is a hydrophilic protein, it must play an important role in lung-tissue water distribution. Only two correlations with $R^2 \geqslant 0.6$ were observed. Figure 5 shows an inverse correlation ($R^2 = 0.760$) between the collagen content and the amplitude of the 2–6 ms T_2 component. This suggested that an increase in the collagen content resulted in a decrease in the nonaqueous component. An inverse correlation with $R^2 = 0.580$ was also found between collagen content and the amplitude of the component for which the T_2 ranged between 80 and 110 ms and accounted for the bulk of lung water content; the data are not shown here. For other NMR properties, no linear correlations with correlation greater than $R^2 = 0.43$ were found. We conclude that the role of the contribution of collagen in the determination of structure and dynamics of lung tissue cannot be considered independently of the other nonaqueous molecular constituents.

Second Moments

For a rigid molecule of known structure, the rigid-lattice second moment is calculable in terms of dipolar couplings between proton pairs (*18*). Due to the presence of motion which is rapid on the proton NMR time scale, $M_2^{-1/2} \approx 10$ μs, the measured second moment is generally less than the rigid-lattice second moment. In the limiting case of rapid isotropic motion on the NMR time scale, the measured second moment approaches zero. For the complex heterogeneous structure of lung, it is not reasonable to estimate the rigid-lattice M_2 value. However, we know that it must be substantially smaller than that for a hydrocarbon chain of methylene (CH_2) groups ($\approx 2 \times 10^{10}$ s^{-2}) (*28*) but likely larger than that estimated for long-chain polysaccharides such as cellulose ($\approx 7 \times 10^9$ s^{-2}) (*35*). The measured average M_2 value for lung tissue of $3.42 \pm (0.25) \times 10^9$ s^{-2} is therefore probably $\frac{1}{3}$ the rigid-lattice value. This implies that long macromolecules undergo considerable anisotropic motion on the NMR time scale. M_2 values measured for lung are not appreciably different from those measured in other biological systems such as membranes (*28*). The twofold increase in M_2 observed as water was removed indicates a substantial reduction in molecular motion upon dehydration (Fig. 3).

Mobile Nonaqueous Signal

From the dehydration study, it was noted that for the fully dehydrated samples, a mobile component with an average

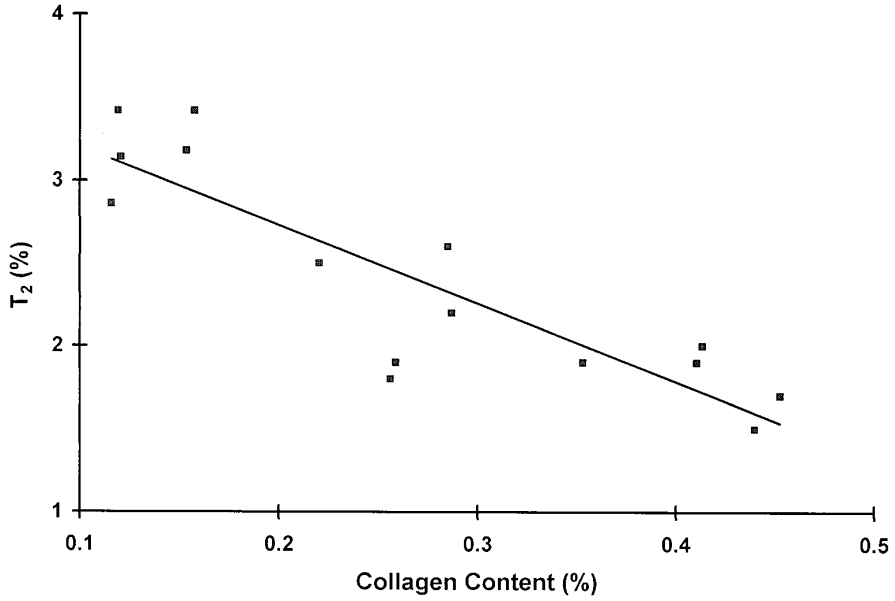

FIG. 5. The amplitude percentage of the 1–10 ms T_2 component plotted as a function of collagen content (collagen mass per dry mass) for each sample.

T_2 of 4 ms remained; this component was also present in wet samples. For this reason, it was hypothesized that the 4 ms T_2 component was due to the nonaqueous mobile protons. This hypothesis was consistent with the NMR spectrum of the fully dehydrated sample which contained a broad line at 6.8 ppm. Figure 6 shows that the signal from the nonaqueous mobile component, L_{nm}, remained relatively constant for most of the dehydration process; $L_{nm}/(S_0 - L_0)$ was about 0.2 ± 0.05 up to a wet/dry ratio of 2. However, for wet/dry ratios lower than 1.8, it followed an abrupt increase. We do not understand this anomalous increase in $L_{nm}/(S_0 - L_0)$ at low hydrations; however, with regard to water content, it has no physiological significance.

NMR Signal Decomposition and Relative Proton Densities

The signal from lung has been separated into components based upon the NMR properties of each component. NMR signal intensities are proportional to the number of contributing protons. Therefore, to relate NMR signal intensities to

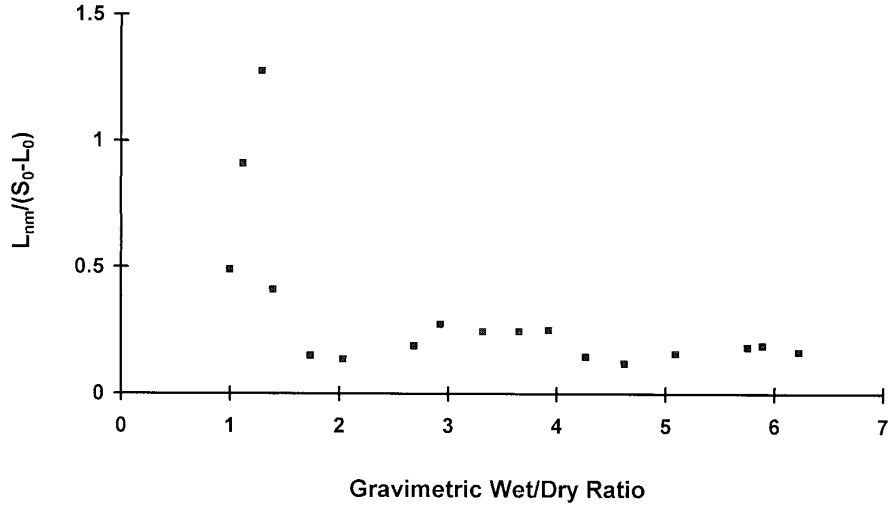

FIG. 6. The nonaqueous mobile signal amplitude divided by the motionally restricted signal amplitude, $L_{nm}/(S_0 - L_0)$, as a function of gravimetric wet/dry ratio.

TABLE 1
Chemical Composition of Lung

Component	Average dry weight (%)	Subcomponent	Average dry weight (%)	Estimated hydrogen content per unit mass
Collagen	30			0.041
Elastin	25			0.074
		Lipids	30	0.105
Whole cell	45	Proteins	25	0.066
		Nonaqueous mobile	45	0.060

sample masses, the hydrogen content per unit mass (ρ) must be known. In this work, two approaches for estimating ρ were developed.

(1) Hydrogen content per unit mass based upon the chemical content of lung. Table 1 shows a list of chemical constituents of lung along with their estimated relative proportion (*36*). For each constituent, the ratio of the numbers of nonexchangeable hydrogens per molecule to the molecular weight was calculated. This provided the relative mass of hydrogen per unit mass. For collagen, it was assumed that hydrogens not bonded to carbon atoms underwent rapid exchange with water on the ^{1}H NMR time scale. Since more than 95% of collagen in lung is types (I) and (III) (*36, 37*), collagen α type (III) (col-bovine) with average molecular weight 9365 and with 3817 nonexchangeable hydrogens was used as the representative collagen. Collagen type (I) and type (III) are homologous proteins. Since elastin is an extremely hydrophobic macromolecule, it was assumed that the hydrogens of elastin do not exchange rapidly with water. The representative macromolecule of elastin was els-bovine with average molecular weight of 64,230 and with 4731 hydrogens.

The amount of hydrogen per unit mass of the whole cell constituents was obtained from (*1*). Some constituents (e.g., cytoplasmic proteins and metabolites) are expected to tumble isotropically at a sufficiently rapid rate ($\tau \approx 10^{-5}$ s) that their dipolar interactions average to zero, giving rise to a narrow line. For this reason, the molecular constituents of lung were divided into motionally restricted and mobile categories and their ρ was estimated separately for each classification. For the relative proportions listed in Table 1, we estimated the relative amounts of hydrogen per unit mass for the motionally restricted nonaqueous, mobile nonaqueous, and water component. When the known collagen content of each sample was included in the calculation (assuming that a decrease in collagen was accompanied by an increase in elastin), the hydrogen content per unit mass for the motionally restricted component, ρ_s, ranged from 0.061 to 0.073 with a mean of 0.066 $\pm$ 0.005. This indicated that the variations in collagen content had a minor effect upon the estimated ρ_s.

(2) Hydrogen content per unit mass based on incremental dehydration. Figure 7 shows $S_0/(S_0 - L_0)$ plotted as a function of gravimetric wet/dry ratio. Assuming that all the mobile signal is from water, the wet/dry ratio is given by

$$\text{wet/dry} = 1 + \frac{L_0}{(S_0 - L_0)} \times \frac{\rho_s}{\rho_w} \times 100\%, \qquad [3]$$

where ρ_w is the hydrogen content per unit mass of water. However, if the contribution from the nonaqueous mobile component to L_0 is taken into account, the wet/dry lung-mass ratio would be related to NMR signal intensities by the equation

$$\text{wet/dry} = 1 + \frac{(L_0 - L_{nm})}{(S_0 - L_0) \times (\rho_w/\rho_s) + L_{nm} \times (\rho_w/\rho_{nm}))} \times 100\%, \qquad [4]$$

where L_{nm} is the signal intensity and ρ_{nm} is the hydrogen content per unit mass of mobile nonaqueous lung tissue. Using a nonlinear functional optimization program (*32*), Eq. [4] was fitted to our results for S_0, L_0, L_{nm}, and gravimetric wet/dry ratio. The values of S_0, L_0, and gravimetric wet/dry ratio were obtained from the incremental dehydration study. The L_{nm} values were set to $0.2(S_0 - L_0)$, based on the dehydration experiments. Due to the rapid and nonlinear increase of L_{nm} at very low wet/dry ratios, only the first 13 points of the 17 dehydrations were used in the fit of Eq. [4] in order to estimate ρ_s and ρ_{nm} (Fig. 7). The resulting values for ρ_s and ρ_{nm} were 0.0717 and 0.045, respectively. The χ^2 for fitting Eq. [4] to the results was $\frac{1}{16}$ that obtained using Eq. [3], underlining the importance and necessity of including L_{nm} in our calculations.

Estimation of Lung Wet/Dry Ratio by NMR

The NMR free-induction decay from each sample was separated into a motionally restricted component with intensity $S_0 - L_0$ and a mobile component with intensity L_0.

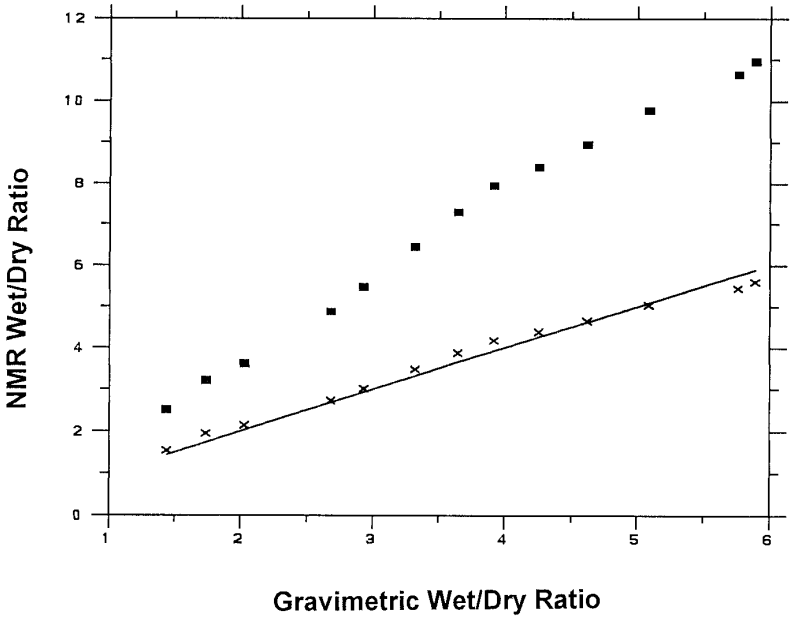

FIG. 7. The NMR wet/dry ratio, taking the nonaqueous mobile component into account (crosses), and $S_0/(S_0 - L_0)$ (filled squares) plotted as a function of gravimetric wet/dry ratio.

Using ρ_s, ρ_w, and L_{nm} derived from chemistry in conjunction with Eq. [4], we estimated the $(\text{wet/dry})_{NMR}/(\text{wet/dry})_G$ ratio to be 1.00 ± 0.08 (Table 2). The values for ρ_s and ρ_{nm} from the dehydration experiment yielded an average $(\text{wet/dry})_{NMR}/(\text{wet/dry})_G$ ratio of 1.00 ± 0.05. The outstanding agreement between the two approaches confirms that the chemical composition of lung portrayed in Table 1 was remarkably accurate.

CONCLUSIONS

In this work, we report on the NMR properties of lung and demonstrate a significant correlation between NMR signal and pulmonary tissue hydration. This paper presents analysis of the entire ^{1}H NMR signal of lung tissue *in vitro*, including the broad-line components. The NMR signal from the nonaqueous mobile protons in metabolites and cytoplasmic proteins, with an average T_2 of 4 ms, was distinguished from the water signal. Discerning these two components, in turn, helped us to obtain excellent agreement between the NMR and gravimetric wet/dry ratio. This indicates that NMR techniques are applicable to the assessment of the regional and whole lung water content.

In conclusion, since many pathologic processes in lung tissue alter water content, this suggests that MR should distinguish normal from abnormal lung tissue. In addition, the differential behavior of the various T_2 compartments within lung tissue offers the capability of characterizing the water environment with MRI, possibly distinguishing inflammatory from fibrotic processes. This characteristic of the microscopic soft-tissue environment cannot be performed by radiologic techniques which measure only lung density.

TABLE 2
Comparison of NMR and Gravimetric Lung Wet/Dry Ratios (n = 21)

ρ_s		Mean	σ
Estimated (chemistry)	$(\text{Wet/dry})_{NMR}$	5.64	0.08
Experimental (NMR)	$(\text{Wet/dry})_{NMR}$	5.65	0.07
	$(\text{Wet/dry})_G$	5.67	0.10
Estimated (chemistry)	$(\text{Wet/dry})_{NMR}/(\text{wet/dry})_G$	1.00	0.08
Experimental (NMR)	$(\text{Wet/dry})_{NMR}/(\text{wet/dry})_G$	1.00	0.05

ACKNOWLEDGMENTS

The authors thank Dr. Karim Qayumi and his group, especially Joanna Sniderman and Chris Gillespie, at the Jack Bell Institute for providing us with the pig lung samples. They also thank Professor Myer Bloom, Dr. Ken Whitttall, and Professor Colin Fyfe for helpful comments. Financial support from the Natural Sciences and Engineering Research Council of Canada is gratefully acknowledged.

REFERENCES

1. M. Bloom, T. Holmes, H. Carolyn, and E. Mountford, *J. Magn. Reson.* **69,** 73 (1989).
2. D. D. Blatter, A. H. Morris, D. C. Ailion, A. G. Cutillo, and T. A. Case, *J. Magn. Reson. B* **102,** 293 (1993).

3. R. A. Christman, D. C. Ailion, T. A. Case, C. H. Durney, A. G. Cutillo, S. Shioya, K. C. Goodrich, and A. H. Morris, *Magn. Reson. Med.* **73,** 6 (1996).
4. R. M. Cotts, M. J. R. Hoch, T. Sun, and J. T. Marker, *J. Magn. Reson.* **83,** 252 (1989).
5. G. Laicher, D. C. Ailion, and A. G. Cutillo, Abstracts of the Society of Magnetic Resonance, p. 609, 1993.
6. C. H. Durney, J. Bertolina, D. C. Ailion, R. A. Christman, and A. G. Cutillo, *J. Magn. Reson.* **85,** 554 (1989).
7. M. R. Estilaei, A. L. MacKay, C. Roberts, and J. Mayo, Abstracts of the Society of Magnetic Resonance, p. 1616, 1995.
8. J. R. Mayo, A. L. MacKay, K. P. Whittall, E. M. Baile, and P. D. Pare, *J. Thorac. Imaging* **16,** 73 (1995).
9. A. G. Cutillo, A. H. Morris, and D. C. Ailion, *J. Appl. Physiol.* **57,** 583 (1984).
10. A. G. Cutillo, A. H. Morris, D. C. Ailion, C. H. Durney, and T. A. Case, *J. Thorac. Imaging* **1,** 39 (1986).
11. F. E. Carroll, J. E. Loyd, K. B. Nolop, J. C. Collins, D. C. Ailion, and S. A. Johnson, *Invest. Radiol.* **20,** 381 (1985).
12. C. E. Hayes, T. A. Case, and D. C. Ailion, *Science* **216,** 1313 (1982).
13. A. H. Morris, D. Blatter, T. A. Case, and A. G. Cutillo, *J. Appl. Physiol.* **58,** 759 (1985).
14. D. C. Ailion, T. A. Case, D. D. Blatter, A. H. Morris, and A. G. Cutillo, *Bull. Magn. Reson.* **6,** 130 (1984).
15. J. R. Mayo, N. L. Muller, B. B. Forester, and M. Okazawa, *Can. Assoc. Radiol. J.* **6,** 281 (1990).
16. P. M. Philips, P. S. Allen, and S. F. P. Man, *J. Appl. Physiol.* **66,** 1197 (1989).
17. S. Meiboom and D. Gill, *Rev. Sci. Instrum.* **29,** 688 (1958).
18. A. Abragam, ''Principles of Nuclear Magnetism,'' Oxford Univ. Press, Oxford, United Kingdom, 1961.
19. C. P. Slichter, ''Principle of Magnetic Resonance,'' 3rd ed., Springer-Verlag, New York, 1990.
20. G. N. Ling and M. Tucker, *J. Natl. Cancer Inst.* **64,** 1199 (1980).
21. G. Antonio, A. H. Morris, K. Ganesan, D. C. Ailion, and T. A. Case, *Magn. Reson. Med.* **12,** 137 (1989).
22. P. A. Bottomly, C. J. Hardy, R. Argesinger, and G. A. Moore, *Med. Phys.* **14,** 1 (1987).
23. S. Shioya, M. Haida, and C. Tsuji, *Magn. Reson. Med.* **8,** 450 (1988).
24. J. R. Mayo, A. L. MacKay, and N. Muller, *Radiology* **177,** 313 (1990).
25. S. Shioya, R. A. Christman, and D. C. Ailion, *Magn. Reson. Med.* **16,** 49 (1990).
26. S. Shioya, M. Haida, M. Fukuzaki, Y. Ono, M. Tsuda, Y. Onta, and H. Yamabayashi, *Magn. Reson. Med.* **14,** 358 (1990).
27. S. Shioya, H. Kolem, D. C. Ailion, and K. C. Goodrich, *Magn. Reson. Med.* **26,** 1 (1992).
28. A. L. MacKay, *Biophys. J.* **35,** 301 (1981).
29. A. L. MacKay, E. Burnell, A. Bienvenue, P. F. Devaux, and M. Bloom, *Biochem. Biophys. Acta* **728,** 460 (1983).
30. H. Stegemann and K. H. Stalder, *Clin. Chem. Acta* **18,** 267 (1967).
31. E. Sternin, *Rev. Sci. Instrum.* **56,** 2043 (1985).
32. F. James and M. Roos, *Comput. Phys. Commun.* **10,** 343 (1975).
33. K. P. Whittall and A. L. MacKay, *J. Magn. Reson.* **84,** 134 (1989).
34. W. T. Sobal and M. M. Pintar, *Magn. Reson. Med.* **4,** 537 (1987).
35. A. L. MacKay, M. Tepfer, I. P. Taylor, and F. Volke, *Macomolecules* **18,** 1124 (1985).
36. G. J. Laurant, *Thorax* **41,** 418 (1986).
37. B. C. Starcher, *Thorax* **41,** 577 (1986).